TU Delft

Delft University of Technology

Development and optical performance tests of the Si immersed grating demonstrator for E-ELT METIS

Navarro, R.; Agócs, Tibor; Venema, L; van Amerongen, A.H.; Rodenhuis, M.; Hoogeveen, Ruud W. M.; Coppens, T; Brandl, Bernhard; Vink, R.

DOI
10.1117/12.2296128

Publication date
2017

Document Version
Final published version

Published in
ICSO 2016, International Conference on Space Optics

Citation (APA)
Navarro, R., Agócs, T., Venema, L., van Amerongen, A. H., Rodenhuis, M., Hoogeveen, R. W. M., Coppens, T., Brandl, B., & Vink, R. (2017). Development and optical performance tests of the Si immersed grating demonstrator for E-ELT METIS. In B. Cugny, N. Karafolas, & Z. S. (Eds.), *ICSO 2016, International Conference on Space Optics: Biarritz, France, 18–21 October 2016* (Vol. 10562). (Proceedings of SPIE; Vol. 10562). SPIE. https://doi.org/10.1117/12.2296128

Important note
To cite this publication, please use the final published version (if applicable).
Please check the document version above.

Copyright
Other than for strictly personal use, it is not permitted to download, forward or distribute the text or part of it, without the consent of the author(s) and/or copyright holder(s), unless the work is under an open content license such as Creative Commons.

Takedown policy
Please contact us and provide details if you believe this document breaches copyrights.
We will remove access to the work immediately and investigate your claim.

This work is downloaded from Delft University of Technology.
For technical reasons the number of authors shown on this cover page is limited to a maximum of 10.

ICSO 2016

International Conference on Space Optics

Biarritz, France

18–21 October 2016

Edited by Bruno Cugny, Nikos Karafolas and Zoran Sodnik

Development and optical performance tests of the Si immersed grating demonstrator for E-ELT METIS

Ramon Navarro

Tibor Agócs

Lars Venema

Aaldert H. van Amerongen

et al.

International Conference on Space Optics — ICSO 2016, edited by Bruno Cugny, Nikos Karafolas, Zoran Sodnik, Proc. of SPIE Vol. 10562, 1056257 · © 2016 ESA and CNES
CCC code: 0277-786X/17/$18 · doi: 10.1117/12.2296128

Downloaded From: https://www.spiedigitallibrary.org/conference-proceedings-of-spie on 12/7/2017 Terms of Use: https://www.spiedigitallibrary.org/terms-of-use

DEVELOPMENT AND OPTICAL PERFORMANCE TESTS OF THE SI IMMERSED GRATING DEMONSTRATOR FOR E-ELT METIS

Ramon Navarro[1*], Tibor Agócs[1], Lars Venema[2], Aaldert H. van Amerongen[3], Michiel Rodenhuis[4], Ruud W. M. Hoogeveen[3], Tonny Coppens[3], Bernhard R. Brandl[4], Ramon Vink[5]

[1]*NOVA Optical Infrared Instrumentation Group at ASTRON, P.O. Box 2, 7990 AA, The Netherlands;*
[2]*ASTRON, the Netherlands Institute for Radio Astronomy, P.O. Box 2, 7990 AA, Dwingeloo, The Netherlands*
[3] *SRON Netherlands Institute for Space Research, Sorbonnelaan 2, NL 3584 CA, Utrecht, The Netherlands*
[4] *Leiden Observatory, Leiden University, P.O. Box 9513, NL-2300 RA, Leiden, The Netherlands*
[5]*ESA, Keplerlaan 1, 2201 AZ, Noordwijk, The Netherlands;*

ABSTRACT

Immersed gratings offer several advantages over conventional gratings: more compact spectrograph designs, and by using standard semiconductor industry techniques, higher diffraction-efficiency and lower stray-light can be achieved. We present the optical tests of the silicon immersed grating demonstrator for the Mid-infrared E-ELT Imager and Spectrograph, METIS. We detail the interferometric tests that were done to measure the wavefront-error and present the results of the throughput and stray-light measurements. We also elaborate on the challenges encountered and lessons learned during the immersed grating demonstrator test campaign that helped us to improve the fabrication processes of the grating patterning on the wafer.

INTRODUCTION

Immersed Gratings (IG)s offer several advantages over conventional front-surface gratings. Since diffraction takes place inside the high-index of refraction material, the optical path difference and angular dispersion are increased proportionally. Consequently, a smaller grating area and beam diameter is sufficient to obtain the same spectroscopic resolution, so a significant reduction of spectrometer volume and mass becomes possible. Using the available expertise and techniques of the semiconductor industry, IGs can achieve higher diffraction efficiency and lower stray light levels. The drawback of IGs is that wave front error of the grating also increases proportionally with the index of refraction.

We build on IG technology that was pioneered by the group of Dan Jaffe in the USA [1] and that we have further developed in the Netherlands for the TROPOMI space spectrometer [2]. Furthermore we make use of knowledge of lithography and process technology as well as optical bonding and fusing techniques that are available at Philips Innovation Services [3]. The detailed production route of the immersed grating is described in [4]. The METIS IG demonstrator is produced using semiconductor equipment for 150 mm diameter wafers. Standard semiconductor lithography techniques and anisotropic etching in silicon are used to create grating grooves with nanometer accuracy and sub-nanometer roughness. Optical bonding is used then to combine the grooved wafer and a silicon prism, followed by thermal fusion to strengthen the wafer-prism bond.

After completion of the IG manufacturing process, its performance is verified against the optical requirements. Interferometric tests measure the wavefront error of both the entry/exit facet as well as the grating surface itself. These measurements are performed with a HeNe laser interferometer operated at 633nm, therefore only air-side measurements could be performed, nevertheless in various orders and in different grating orientations. The wavefront error budget of the complete IG is disclosed, including how the wavefront error of various sources were deduced and calculated from the measurements.

The optical arrangement and results of the IG throughput measurements with a modified infrared Fourier Transform Spectrometer (FTS) are presented. The measurement gave insight into the diffraction efficiency of the grating knowing the AR coating characteristics of the entrance/exit surface. Throughput was measured over the complete operational wavelength range of the METIS spectrograph, between 2.9μm and 5.3μm.

The dedicated mounting arrangement and results of the BRDF (Bidirectional Reflection Distribution Function) measurements, performed with a Complete Angle Scatter Instrument (CASI), are presented in spectral and spatial direction. Defects observed after optical contacting and bonding (between the prism and wafer) were investigated as well. We present the lessons learnt during the IG demonstrator test campaign and elaborate on the challenges that we encountered, especially during the wavefront error measurements that led us to investigate further and improve the fabrication processes of the grating patterning on the silicon wafer.

*navarro@astron.nl Tel +31 521 505 235

Downloaded From: https://www.spiedigitallibrary.org/conference-proceedings-of-spie on 12/7/2017 Terms of Use: https://www.spiedigitallibrary.org/terms-of-use

METIS IMMERSED GRATING

METIS is the Mid-infrared E-ELT Imager and Spectrograph, which will provide outstanding observing capabilities, focusing on high angular and spectral resolution on the largest telescope on Earth. The common fore optics re-images the focal plane of the EELT inside METIS and provides the following essential functionalities: calibration, chopping, image de-rotation, thermal background and stray light reduction. METIS consists of two diffraction-limited imagers, providing also low and medium resolution long slit spectroscopy, operating in the LM and NQ bands respectively and one Integral Field Unit fed diffraction-limited high-resolution spectrometer. This high resolution spectrometer operates in the L/M bands, in a cryogenic environment (<85 ºK), and it provides a spectral resolution of 100000 at 4.65μm. It consists of pre-optics, an Integral Field Unit and main optics. The spectral dispersion element is the Immersed Grating and orders are separated by a pre-disperser [5] [6].

Considering the difficulties of the manufacturing a large classical echelle grating, it was decided to investigate the possibility to employ an IG in the heart of the spectrometer. Based on the wavelength range (2.9 μm - 5.3 μm) Si is ideally suited as immersion material. Apart from the good transmission, single crystal Si also has beneficial anisotropic etching characteristics that allows for tailoring the groove profile to the specific grating requirements. The grating is obtained via etching into the Si with the surface cut along the <100> crystal plane. The grooves thus have a natural blaze angle close to 54.7 degrees depending on the anisotropic etch ratio. The angle of incidence on the grating is close to this blaze angle. The grating is positioned at the bottom of a Si prism (Figure 2). The grating is produced on a regular Si wafer that is bonded to the bottom surface of a Si prism. The light enters and exits the prism through the same facet. The METIS IG demonstrator was manufactured successfully.

Fig. 1. The METIS Immersed Grating. Left: Immersed grating principle: light enters the prism through a polished entrance facet (black arrows); after diffraction at the grating facet the dispersed light leaves the prism through the entrance facet (red and blue arrows). Center: 3D drawing of the METIS IG, with the grating wafer detached from the prism. Right: The completed METIS IG demonstrator is ready to start the test campaign.

EFFICIENCY MEASUREMENTS

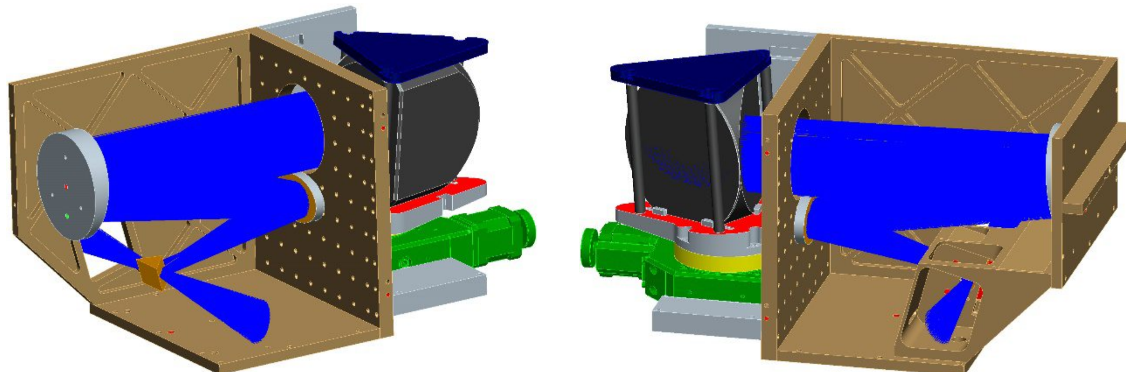

Fig. 2. A Fourier Transform Spectrometer setup with 60mm collimated beam is developed in order to measure the efficiency of the METIS IG demonstrator. Optical beams are blue, IG is dark grey, rotation stage is green.

Using PCGrate, the grating pattern was modelled and the diffraction efficiency was calculated for TM and TE polarization using representative values for the shape of the grating and the off-Littrow angle in the setup. The AR coating was also modeled and taken into account to calculate the nominal throughput of the IG. After the optical bonding and fusing, defects were detected in the prism to wafer interface within the requirement area and IR inspection revealed that 3.5% of the performance area is affected by these defects. In order to see the expected performance, IG throughput without defects is shown as well.

Downloaded From: https://www.spiedigitallibrary.org/conference-proceedings-of-spie on 12/7/2017 Terms of Use: https://www.spiedigitallibrary.org/terms-of-use

The efficiency is measured using a modified Varian 7000e Fourier Transform IR Spectrometer (FTS), with a wavelength range from 200nm to 28 micrometer, covering the entire METIS wavelength range (2.9µm - 5.3µm). A gold coated mirror was used as a reference sample. A dedicated FTS setup was developed to measure the throughput of the IG in a relevant way. A specially developed relay system collimates the light into a 60mm diameter beam that can be used to measure the sample in reflection. The IG was placed on a motorized rotation stage that was used to scan the complete wavelength range of interest.

In the figure 3 the throughput or efficiency is shown for 2.7-3.8µm and 3.8-5.5µm. The top line #1 shows the modelled diffraction efficiency of the grating, line #2 includes the modelled AR coating, line #3 shows the calibrated measurement data corrected for the effect of the defected areas and finally line #4 depicts the calibrated measurement data. The difference between simulations and measurement results (#2 and #3) is best in the 3.3-4.6µm wavelength range, where the difference is still 7-8%. Outside this range the efficiency gradually decreases and at the edges of the wavelength range the IG underperforms by 12-13%. It is not known what causes the degradation of the throughput at these wavelength ranges. If it is presumed that a defect free IG can be manufactured, the highest throughput will be still only 76-77%, not reaching the 80% requirement.

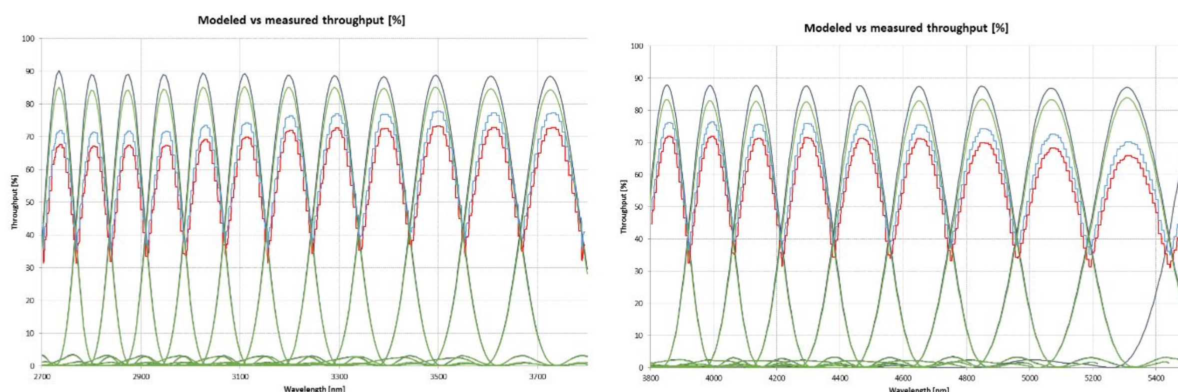

Fig. 3. Throughput of the IG is shown for the 2.7µm – 3.8µm – 5.5µm wavelength range. Going from the curve with the highest peaks towards the curve with the lowest peaks, line #1 shows the modelled diffraction efficiency of the IG, #2 shows the modelled diffraction efficiency + AR coating, #3 shows the calibrated measurement data without the effect of the defected areas and #4 depicts the calibrated measurement data.

Figure 4 shows the logarithmic scaled throughput for the 0 degree IG measurements. The noise is at the 0.1% throughput level. There are no distinguishable small ghosts, satellites visible.

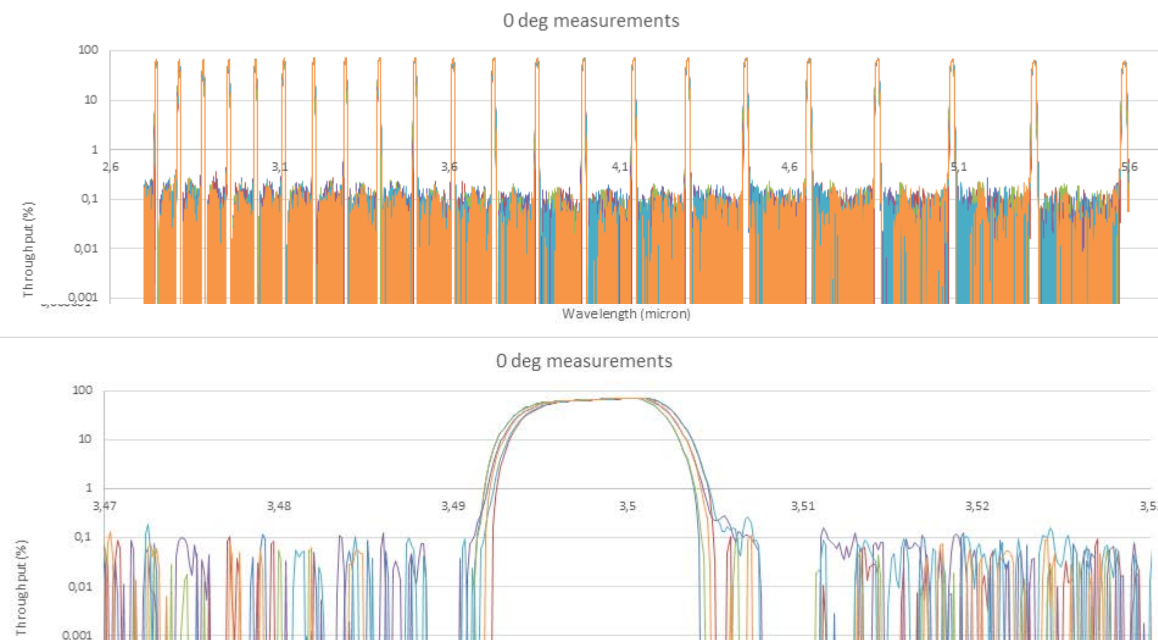

Fig. 4. Efficiency measurement results of the METIS IG demonstrator on a logarithmic scale. The complete wavelength range at the top, at the bottom zoomed to 3.47-3.53 µm range. Ghosts are below the ~0.1% level.

Downloaded From: https://www.spiedigitallibrary.org/conference-proceedings-of-spie on 12/7/2017 Terms of Use: https://www.spiedigitallibrary.org/terms-of-use

BIDIRECTIONAL REFLECTION DISTRIBUTION FUNCTION MEASUREMENTS (BRDF)

BRDF (Bidirectional Reflection Distribution Function) is measured by the SMS CASI (Complete Angle Scatter Instrument) setup at ESA. It uses a 3.39 micron (HeNe) laser as a non-destructive probe. The sample is mounted on stages capable of moving in X and Y and/or rotation. The incident angle can be set to any angle up to ~85° from surface normal. The detector sweeps around the sample in the incident plane measuring scattered and specular light. BRDF describes the directional dependence of the reflected optical energy. It is a fundamental optical property and describes the energy scattered into the hemisphere above a reflective and/or scattering surface as a function of the angle of the incident radiation and the scatter angle. The measurement is done both in spectral and spatial directions. The METIS IG is positioned in a permanent mount and from that moment, only this mount is used to handle the IG. A dedicated mechanical structure, containing the permanent mount and the IG, is also designed in order to measure the defects that are present in between the wafer and the prism. First the complete mechanical arrangement is aligned with respect to the coordinate system of the CASI system, subsequently the mechanical structure is adjusted in order to position the IG in several discrete orientations, where laser light hits dedicated defects without any further alignment, see figure 5.

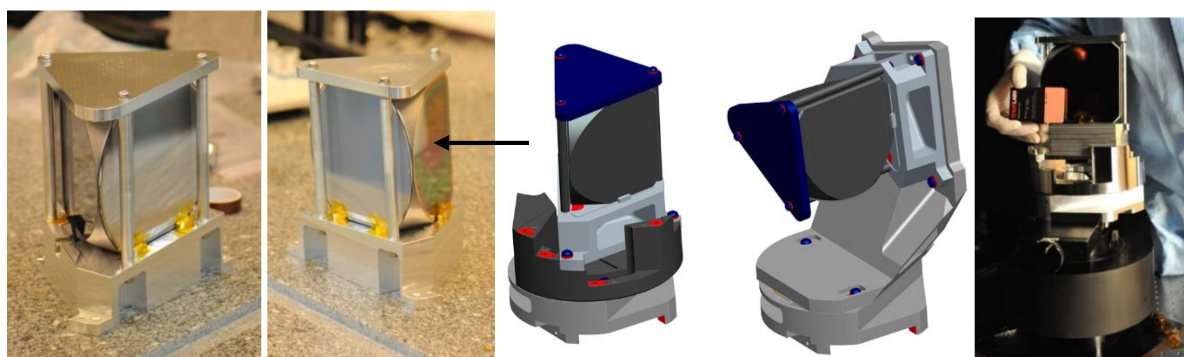

Fig. 5. METIS IG on its permanent mount. The arrow in the 2nd figure shows the entrance surface of the prism. The CAD model of the IG mount is shown in the 3rd (measurement in spectral direction) and 4th (spatial direction) picture. On the far right, the setup is shown in the lab during alignment.

BRDF measurements are performed in immersion, centred on the 33rd order (3.39 µm). The Angle Of Incidence (AOI) of these measurements is defined by METIS spectrograph AOI configuration, where the exiting 33rd order is displaced horizontally 4.5° from the input beam. This angular position becomes the "0°" position in the BRDF figure below. A second measurement is done with a slightly different IG rotation (2.5° from the nominal).

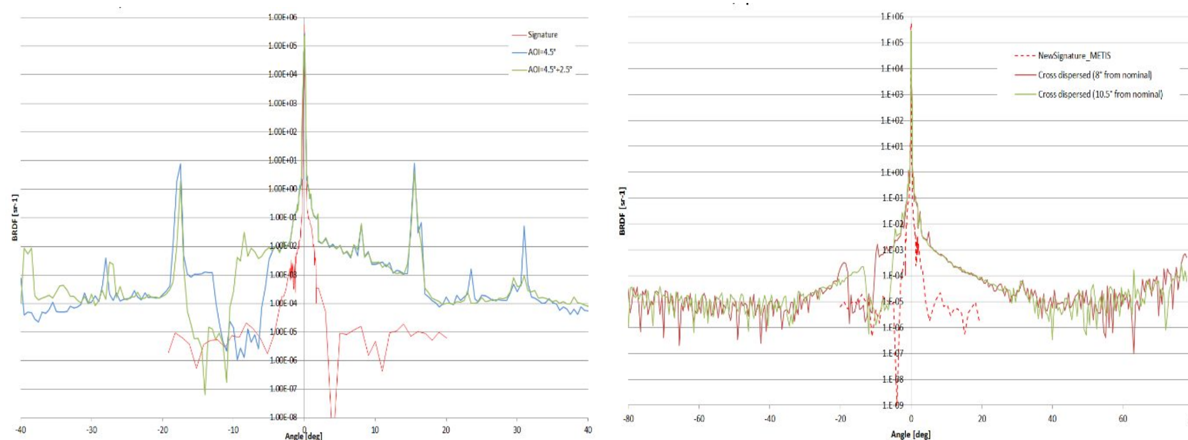

Fig. 6. BRDF of the non-defected area in spectral direction (left) and spatial direction (right).

Both in the spectral and spatial direction the BRDF of the IG is very good, see figure 6. In spectral direction the strongest peaks are 6-7 orders of magnitude lower than the parent peak. The neighbouring orders are also visible in the measurements. Halfway between the parent peak and the neighbouring orders there are smaller satellites that can be ghosts arising from periodic errors in the grating pattern. In spatial direction the result is the same as in the spectral direction, the strongest peaks are 6-7 orders of magnitude lower than the parent peak. The BRDF on defected and non-defected areas is the same and thus it seems that the defects don't have any negative effect on the scattering characteristics of the IG.

Downloaded From: https://www.spiedigitallibrary.org/conference-proceedings-of-spie on 12/7/2017 Terms of Use: https://www.spiedigitallibrary.org/terms-of-use

WAVE FRONT ERROR MEASUREMENTS

The METIS Wave Front Error (WFE) requirements are derived from the specification that the METIS spectrometer must be diffraction limited at the shortest wavelength (2.9 µm). Using the WFE budget of METIS we derived 100nm RMS WFE for the IG, which should be further broken down into the following measurable contributors: #1: Prism Front Surface, #2: Prism Back Surface, #3: Wafer Thickness variation and finally #4: Grating Wave Front Error reflected at air side, see figure 7.

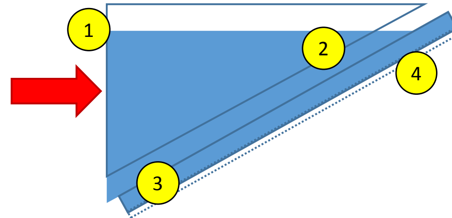

Fig. 7. IG WFE contributors, originating from the prism and wafer. #1 and #2 are surface WFE of the prism. #3 is the wafer thickness variation. #4 is the grating WFE. To obtain the total infrared WFE, all parameters have to be multiplied by the index of refraction of the Si material (n= 3.4), and parameters #1, #2 and #3 have to be multiplied by a factor of 2 (double pass). The geometric angle of incidence must also be taken into account.

On the Prism Front Surface the incoming and returning beams do not fully overlap, therefore these 2 air-surface interfaces can be treated as semi-independent (factor √2 instead of 2). The incoming and returning beams fully overlap on the Prism Back Surface, therefore this contribution is doubled. The same applies for the Wafer Thickness variation. The geometric angle of incidence must be taken into account as well. On the immersed side the Grating Wave Front Error has an effect that is the index of refraction times higher than on the air side of the grating. The Grating WFE (#4) can be broken down into 4 sub categories: Grating line width variations after Reactive Ion Etching, of which half is visible in the grating front surface (#4A), Lithography Distortion Errors (#4B, low order Zernike errors such as: tilt, piston, focus, astigmatism at the right angle, will be corrected in the alignment and are not a problem for WFE), Lithography stitching errors (#4C, absent for currently used full field technology), and Mask writing errors (#4D, taking into account the magnification factor). See Table 1.

Table 1. IG WFE contributors. See description and figure 7 for an explanation of the # items. The values for the individual contributors are listed in black. The calculated contribution to the IG WFE in Littrow is listed in blue.

	Immersed Grating WFE Budget item number	Grating line position error 1σ RMS [nm]	Individual surface error 1σ RMS [nm]	Air side Special case: +WFE +52 +WFE -52 [nm]	Air side Special case: +WFE +52 -WFE -52 [nm]	Air side Grating WFE RMS [nm]	Immersed Grating WFE RMS [nm]
	Total			**48**	**24**	**27**	**98**
Prism Front Surface	#1		10				34
Prism Back Surface	#2		10	11		11	39
Wafer Thickness variation	#3		10	11		11	39
Grating Wave Front Error (@ air side)	#4	13		18	12	22	73
Line width variation (half in front surface)	#4A	22		18		18	62
Lithography Distortion Errors	#4B	6			10	10	34
Litho stitching errors (not for MA8)	#4C	0			0	0	0
Mask writing errors (magnification factor)	#4D	4			6	6	22

We don't have access to an infrared interferometer. Interferometric measurements have been performed at 633nm to characterize the WFE of the entrance and grating surfaces from air-side using a WYKO 6000 interferometer. Measurements were performed in both the positive and negative grating orders close to the Littrow configuration e.g. order +52nd and -52nd. In addition, the 0th order was measured, where the interferometer is effectively measuring the flat dams between the grating grooves and thus it is a measure of the flatness of the grating surface as a whole. Determined from the WFE budget, the WFE for orders close to Littrow should be smaller than 27nm RMS and in 0th order smaller than 16nm (quadratically adding #2 and #3). These values ensure that the overall METIS IG demonstrator WFE is smaller than 100nm RMS, which is the requirement.

Figure 8 Shows the WFE measurements for +52nd and -52nd orders. The WFE over the footprint is 520 nm RMS after subtracting the focus term, nearly a facto 20 higher than the design value of 27 nm RMS. The WFE measurement in the 0th order shows a WFE of 54 nm RMS (not shown). While this is still approximately three

Downloaded From: https://www.spiedigitallibrary.org/conference-proceedings-of-spie on 12/7/2017 Terms of Use: https://www.spiedigitallibrary.org/terms-of-use

times the required value, it is clear that the overall flatness of the grating surface (a combination of the surface flatness of the prism and the Total Thickness Variation (TTV) of the wafer) is not the source of the extremely large WFE seen in the dispersed orders. Prime suspect for the high WFE is the grating pattern itself. This has been further investigated as is explained in figure 8 and reference [7].

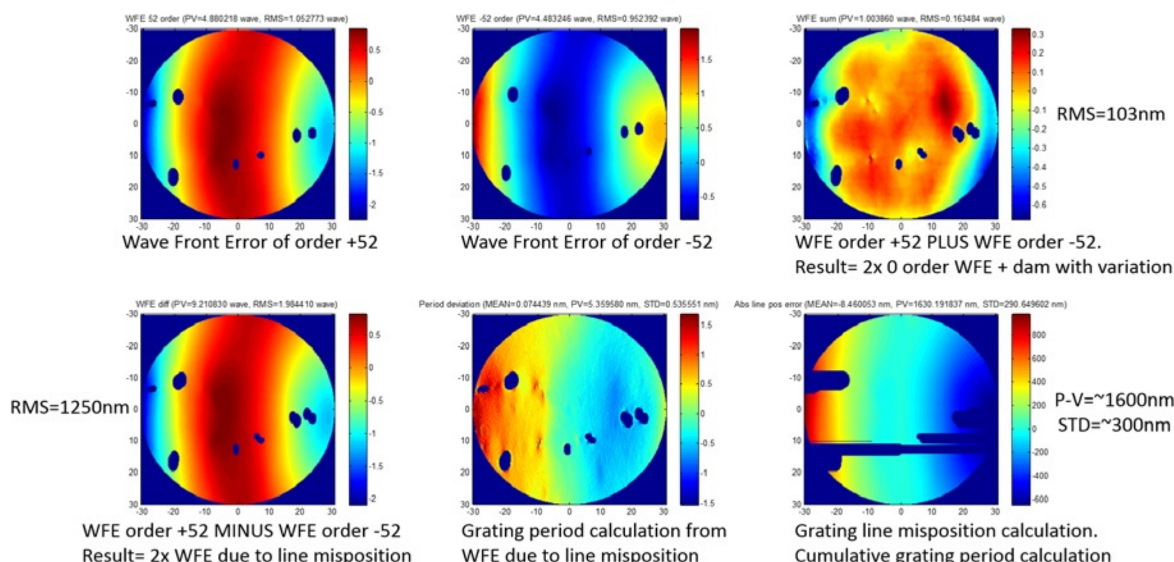

Fig. 8. WFE of the METIS IG demonstrator over the spectrograph clear aperture (60 mm diam. round beam). The WFE measured in +52nd and -52nd order are shown top-left & top-centre. At top-right is the sum of WFE in + and – order, at bottom-left the difference, see also the columns marked 'Air side special case' in table 1. The top-right should be equal to twice the WFE measured in 0 order, plus dam width variation effects, items #2, #3 and #4A from the budget. The measured value corresponds to the expectation (0 order measures 54nm RMS). The bottom-left should be equal to double the WFE resulting from line positioning errors, items #4B, #4C and #4D in the error budget. From this WFE the period deviation is calculated (bottom centre) as well as the absolute line position error (bottom right). The line position error is around 1600 nm peak-to-valley.

The METIS IG demonstrator WFE is far out of specification and dominated by the grating line positioning errors as can be seen in the bottom row of images in Figure 8. A root cause analysis has been performed, with new wafers being processed from scratch, verifying the process at every step and where possible quantifying every possible WFE contribution. The WFE of wafers that were fully processed in this root cause analysis, perform 30 times better and would meet the specifications in table 1, see figure 9.

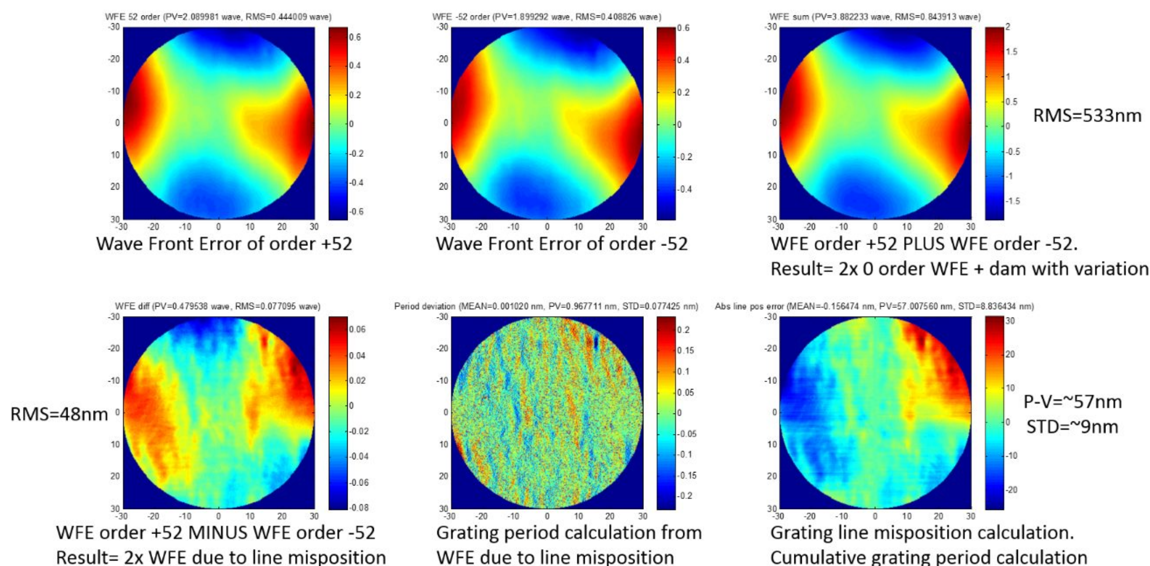

Fig. 9. WFE results of the fully processed root cause analysis wafer, limited to the METIS spectrograph clear aperture (60 mm diam. round beam). The information in the different panes is the same as in Figure 8.

Downloaded From: https://www.spiedigitallibrary.org/conference-proceedings-of-spie on 12/7/2017 Terms of Use: https://www.spiedigitallibrary.org/terms-of-use

For this processed wafer, the RMS value of 9nm for the line positioning error is according to specifications. The measured WFE RMS value of 48nm (bottom left image) is twice the expected value calculated for this special case in the error budget. The measurement however suffers from additional errors sources, such as the varying wafer clamping to measure both order +52 and -52. The actual root cause for the far out of spec WFE of the METIS IG demonstrator has not been found, nevertheless we have isolated the error to the grating pattern on the wafer and we have demonstrated to be able to produce wafers with grating patterns that meet the specifications.

For 3 wafers the total thickness variation has been measured over the clear aperture, while the wafers were optically bonded to a reference flat. When correcting only for tilt and power terms, the average RMS TTV is 16.7nm with a spread of 1nm 1σ. In the METIS spectrometer we can correct one astigmatism term as well, if it is oriented in a favourable direction (spatial-spectral). When correcting for astigmatism terms as well (any direction), the average RMS TTV is 11.8nm with a spread of 3nm 1σ. The TTV specification is 10nm (budget item #3), so these values are out of spec. However the impact of the measured TTV values on the total WFE budget would be mild: anywhere between 3 to 12nm on top of the 98nm nominal WFE.

DEFECTS

A separate issue for the METIS IG demonstrator is the appearance of defects during the bonding process. Bonding is done by optical contacting and this procedure is performed in vacuum with extremely clean surfaces. The observed defects could be caused by particles between the wafer and the prism, however a contamination source or outgassing could not be ruled out. The total surface area affected by these defects is 3.6%, which is significantly larger than the specification of 0.5%. The fear is that these defects could grow in size by a combination of a vacuum environment and thermal cycling. This has been tested and after 2 months under vacuum and 8 thermal cycles between 295K and 80K we see no evidence of a grow in size of the defects, see figure 10.

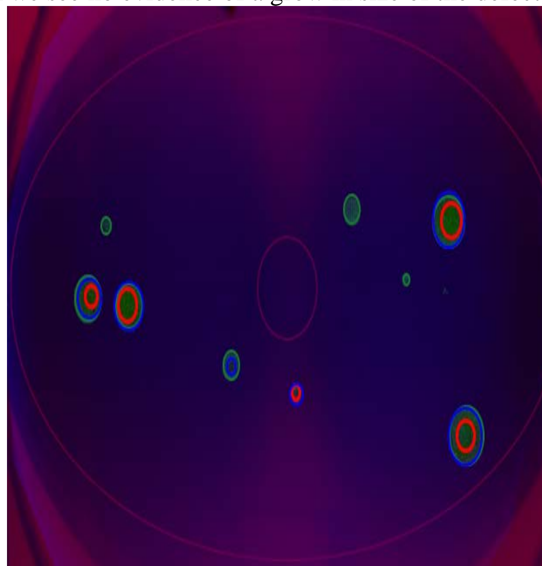

Fig. 10. Defects in the METIS IG demonstrator appear as ovals due to the inclined viewing angle. Bright red ovals indicate defects present after the bonding process. Green ovals indicate defects present after the fusing process, Blue ovals indicate defect bumps observed with the interferometer after 2 months under vacuum and 8 thermal cycles between 295K and 80K. The large pale red circle represents the METIS optical footprint on the IG.

The thermal cycling created an opportunity to test the hypothesis that there is no trapped gas in the voids between the wafer and the prism. This can be tested by measuring the height of the defect bumps at a temperature of 80K and 295K. The expected volume shrink due to gas pressure is a factor of 3.7, which would result in a bump height difference of the same factor. The observed difference is less than a mere 3%, indicating that trapped gas is not a likely case for the defects, and that defects are probably caused by particles.

In the same test sequence the difference in defect bump height was measured in vacuum and at ambient pressure. On average the bump peak height was 21% smaller when a 1Bar pressure was pushing against the surface. The shape of the bumps under atmospheric pressure is noticeably steeper than under vacuum, supporting the theory that there is a particle at the centre of each defect. The force from ambient pressure on such a particle would depend on the size of the defect and would be in the range of 3 to 40N.

Downloaded From: https://www.spiedigitallibrary.org/conference-proceedings-of-spie on 12/7/2017 Terms of Use: https://www.spiedigitallibrary.org/terms-of-use

CONCLUSIONS

In the current paper we discussed the results of the METIS Immersed Grating demonstrator measurements that were performed in order to verify the optical requirements of the component.

The measured efficiency of the IG is 72-73% at the peaks in the 3.2-4.0µm wavelength range. This is 7-8% lower than the >80% requirement. At the short and long edges of the wavelength range the efficiency reduces to 68% and 66% respectively. It is not known what causes the degradation of the throughput at these wavelength ranges. A defect free IG would increase the efficiency by 3.6%. This is still 7-8% lower than the expected 84-85% for a perfect diffraction grating with a perfect (as designed) AR coating, which could be caused by an imperfect grating pattern and/or AR coating. It is believed that with the improved WFE of the immersed grating, the diffraction efficiency will be increased as well.

Regarding scattered light characteristics of the METIS IG demonstrator, both in the spectral and spatial direction the BRDF is very good. In spectral direction the strongest peaks are 6-7 orders of magnitude lower than the parent peak. The neighbouring orders are also visible in the measurements. Halfway between the parent peak and the neighbouring orders there are smaller satellites that can be ghosts arising from periodic errors in the grating pattern. In spatial direction the result is the same as in the spectral direction, the strongest peaks are 6-7 orders of magnitude lower than the parent peak. The BRDF on defected and non-defected areas is the same and thus it seems that the defects don't have any negative effect on the scattering characteristics of the IG.

From the WFE measurements we concluded that in the orders close to the Littrow configuration, the METIS IG demonstrator has a WFE that is more than an order of magnitude higher than expected and required. Due to the significantly large WFE of the METIS IG demonstrator, a root cause analysis has been performed, creating new grating wafers. The observed excess WFE in the METIS demonstrator IG can be explained by an aberration of the grating line pattern. The aberration has two components: a varying error of the grating period and a curvature of the lines. The peak-to-valley line position error required to produce the observed WFE is on the order 1.2 µm. In the full re-run of the photo-lithographic process of the METIS IG, wafers have been produced with line position errors that are well below the requirement. The total thickness variation has been measured for 3 wafers. With these wafers, correctly bonded to a prism of the same quality as that used for the demonstrator IG, this would have yielded an IG with an overall WFE performance of 101 to 110nm, slightly above the 100 nm RMS specification.

The METIS IG demonstrator suffers from defects in the optical bond between the wafer and prism. Tests show that these defects do not grow as a result of thermal cycling under vacuum. Measurements suggest that the defects are probably caused by particles between the wafer and the prism.

We believe that we understand the performance of the METIS IG demonstrator sufficiently well to produce a new Immersed Grating that will be very close to specification.

ACKNOWLEDGEMENTS

The immersed grating development project has been made possible by Netherlands Organization for Scientific Research (NWO) via the ESFRI-project grant number 184.021.006.

REFERENCES

[1] Marsh, J. P.; Mar, D. J.; Jaffe, D. T., "Production and Evaluation of Silicon Immersion Gratings for Infrared Astronomy", Appl. Opt., 46, 3400 (2007).

[2] A. H. van Amerongen, H. Visser, H. J. P. Vink, T. Coppens, R. W. M. Hoogeveen., "Development of immersed diffraction grating for the TROPOMI-SWIR spectrometer", Proc. SPIE 7826 (2010).

[3] J. Haisma, B. A. C. M. Spierings, U. K. P. Biermann, and A. A. van Gorkum, "Diversity and feasibility of direct bonding: a survey of a dedicated optical technology", Appl. Opt. 33, 1154-1169 (1994).

[4] Amerongen, A., H., et al, "Development of Silicon immersed grating for METIS on E-ELT", Proc. SPIE 8450-100 (2012).

[5] Agócs, T., et al., "Preliminary optical design for the common fore optics of METIS", Proc. SPIE 9908-360 (2016).

[6] Brandl, B. R. et al., "Status of the mid-infrared E-ELT imager and spectrograph METIS", Proc. SPIE 9908-74 (2016).

[7] Agócs, T., et al., "Optical tests of the Si immersed grating demonstrator for METIS", Proc. SPIE 9912 (2016).

Downloaded From: https://www.spiedigitallibrary.org/conference-proceedings-of-spie on 12/7/2017 Terms of Use: https://www.spiedigitallibrary.org/terms-of-use